HELSINKI UNIVERSITY OF TECHNOLOGY
Faculty of Electronics, Communications and Automation
Department of Micro and Nanosciences

Shuo Li

Optimization of precursor pulsing in atomic layer deposition

Master's Thesis submitted in partial fulfillment of the requirements of the degree of Master of Science in Technology.

Espoo, Finland, 12.12.2008

Supervisor: Prof. Harri Lipsanen
Instructor: M.Sc. Markus Bosund

ACKNOWLEDGEMENTS

This thesis has been carried out in both the Nanotechnology group and the Photonics group at the Department of Micro and Nanosciences of Helsinki University of Technology. The work presented is a preliminary part of a project funded by the Finnish Funding Agency for Technology and Innovation (Tekes), *Novel nanofabrication methods for specialty optical fibers*.

I would like to thank Prof. Harri Lipsanen and Prof. Seppo Honkanen for giving me the opportunity to work in their groups, and the various motivating conversations，as well as their supervision of my work. To my instructor Markus Bosund (M.Sc.), I owe special mention for his continued guidance, support, and especially patience.

Special thanks are acknowledged to Mr. Markku Rajala (M.Sc.), Mr. Sampo Ahonen (M.Sc.) and Mr. Veli-Matti Airaksinen (Ph.D.) for their initial encouragement and continuous support to my studying in Finland. I am also thankful to Mr. William Martin (M.A.) for his invaluable advice and preparation of the manuscripts. I would like thank to all the staff members at the Department of Micro and Nanosciences, who have been highly supportive during my thesis work.

Finally, I thank my parents, Mr. Xiufeng Li (父亲) and Mrs. Fengying Wang (母亲), for the years of care and encouragement. Also thanks for every happy moment brought by my girlfriend Ms. Miao Wang.

Espoo, 12.12.2008

Shuo Li

Helsinki University of Technology **Abstract of the Master's thesis**

Author: Shuo Li

Title of Thesis: Optimization of precursor pulsing in atomic layer deposition

Date: 12.12.2008 Pages: 54

Department: Department of Micro and Nanosciences

Professorship: Micro and Nanosciences Code: S-129

Supervisor: Prof. Harri Lipsanen

Instructor: M.Sc. Markus Bosund

In this work aluminum oxide (Al_2O_3) and tantalum oxide (Ta_2O_5) films are grown by atomic layer deposition (ALD) on silicon substrates. The research was performed at Micro and Nanosciences Department of Helsinki University of Technology. The effect of precursor pulsing time and pulsing method on film growth rate, mean thickness and thickness variations was studied. The film thickness was measured with ellipsometry.

The modeling of precursor pulsing time was presented. The simulation of trimethylaluminum (TMA) pulsing pressure with different pulsing time was carried out. The results indicated that the pressure before the pulsing valve decreases to a steady state if the valve open time was long enough.

In TMA and H_2O optimization experiments, the growth rate of 1.2 Å/cycle and thickness variation of 0.4% were achieved with 100 ms H_2O pulsing time at a temperature of 220℃. In $TaCl_5$ and H_2O experiments, 0.8 Å/cycle growth rate and 4.6% thickness variation obtained with 25 ms $TaCl_5$ pulsing time at 200℃. In the $TaCl_5$ pulsing mode optimization experiments, the same growth rate of 0.8 Å/cycle was acquired with booster pulse mode and combination pulse mode.

Keywords: atomic layer deposition, precursor pulsing, tantalum oxide

Contents

1 Introduction

Atomic Layer Deposition (ALD) is a chemical vapor deposition technique which is based on successive, surface-controlled reactions from the gas phase to produce thin films with good conformality and process controllability [1,2]. ALD process was firstly introduced in the early 1970s by Tuomo Suntola. The original name was *Atomic Layer Epitaxy (ALE)* at that time [3] and the aim was to produce flat panel displays based on thin film electroluminescence [4]. In addition, ALD has the capability to coat complex shapes with a conformal material layer of high quality [1]. Furthermore, ALD can make accuracy thickness control, facile doping, large area uniformity, and pinhole free film [2].

ALD processes have been developed to manufacture many types of solid inorganic materials for a wide range of applications, such as oxides, nitrides, sulphides, selenides, tellurides and pure elements. Among these materials, oxides have been the type most often investigated. Typically, Al_2O_3 can be used as a dielectric, protective or ion barrier layer in electronic and optoelectronic devices [5]. Ta_2O_5 has a high dielectric constant that makes it a promising candidate for capacitor insulators in high-density dynamic access memories (DRAM) and insulating layer in thin film electroluminescent [6].

The goal of this study was to identify the optimal conditions for a reproducible growth of high quality Al_2O_3 and Ta_2O_5 films. This is done by varying the experimental

parameters and observing their effect on film growth rate and film properties. In ALD technology, the precursors are pulsed onto the substrate alternately [7]. Therefore, the sequential surface reaction processes are saturated and the film growth is self-limiting.

In the course of this work, Al_2O_3 and Ta_2O_5 films are taken as examples and deposited with different precursor pulse length and pulsing modes. The objectives of the work are: 1) to model and simulate the influence of the precursor pulse length on precursor dose ; 2) to optimize the precursor pulse length in the Al_2O_3 and Ta_2O_5 ALD growth process; 3) to optimize the precursor pulse method in the Ta_2O_5 ALD process. The work was carried out in the Department of Micro and Nanosciences using the cleanroom and facilities at Micronova.

The thesis is organized as follows. In chapter two, the basic features of ALD are provided; Chapter three focuses on the precursor chemistry. In chapter four, the important ALD technology related issues are presented. The modelling of precursor pulsing are described in chapter five; In chapter six, the measurement method of ellipsometry is described. In chapter seven, the experimental methods are discussed in details. The results of the experiments and measurement dates are analysed in chapter eight. Finally in the last chapter, a summary of the work is given together with proposals for future research.

2 Basic features of ALD

This work will be the first Master's thesis about ALD process optimization published in English from the Department of Micro and Nanosciences, for this reason this chapter will give an overview about the basic features of ALD，which include: the working principle of ALD, surface saturation and self-limiting reactions, ALD window as well as the advantages and limitations of ALD.

2.1 The working principle of ALD

In an ideal ALD growth process, different precursors are pulsed alternately onto the substrate surface in different steps. The non-reacted reactants and the reaction by-products are removed by the following inert gas purge step. This feature keeps the precursors strictly separated from each other in the gas phase. As a result, there is only the reaction of a gaseous compound reactant with the solid surface in the ALD process, which is defined as the gas-solid reaction. Considering a typical two-reactant ALD process, there are usually four steps in each cycle growth as follows [8]:

Step # 1 Pulse first precursor A and self-terminating reaction on the substrate surface

Step # 2 Purge to remove the non-reacted reactants and the reaction by-products

Step # 3 Pulse second precursor B and self-terminating reaction again

Step #4 Purge to remove the non-reacted reactants and the reaction by-products again

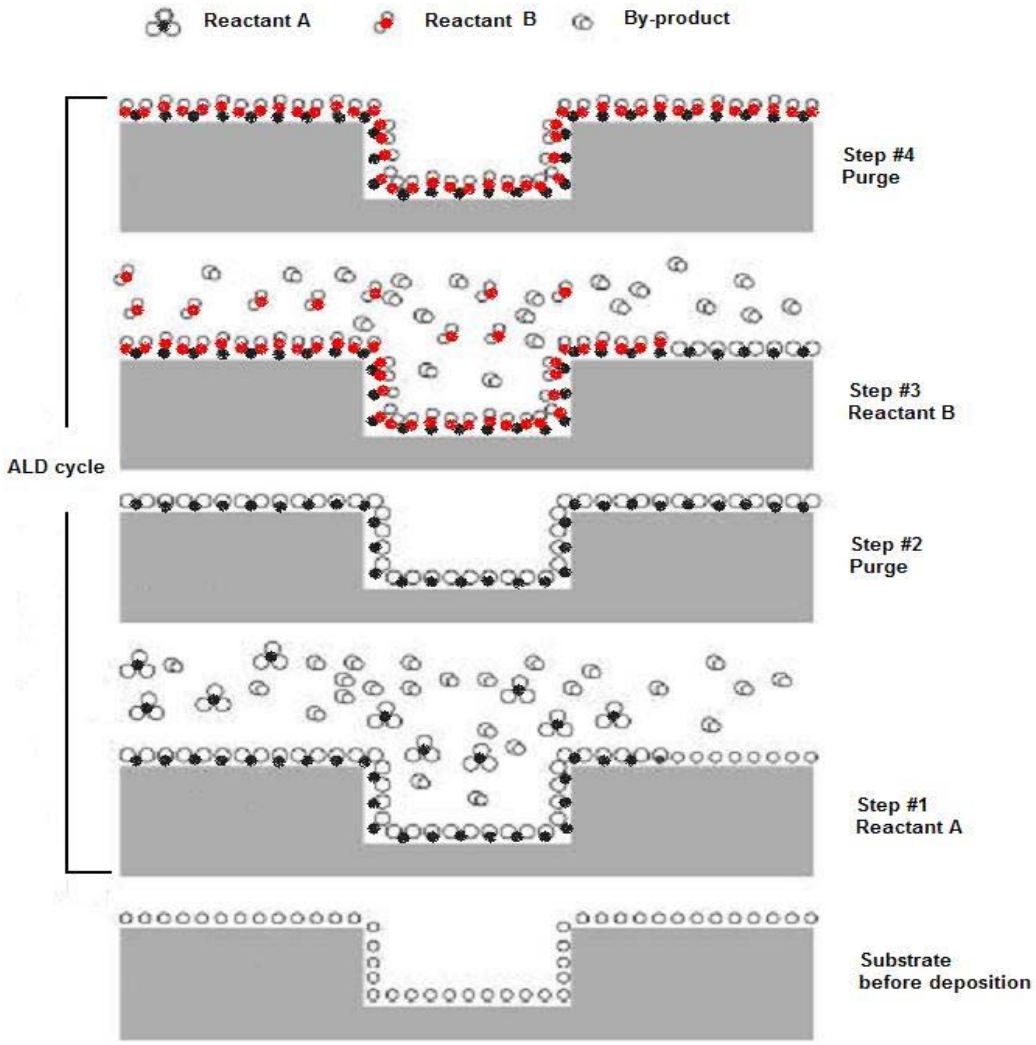

Figure 1 *Schematic illustration of one ALD reaction cycle.*

One ALD reaction cycle is explained schematically in ***Figure 1***. Each reaction cycle will add a given amount of material to the substrate surface. In order to deposit a material layer, reaction cycles are repeated sequentially until the desired amount of material has been grown [9].

Growth rate is defined as the amount of material deposited one reaction cycle. The unit is usually Å/cycle. The film growth per cycle is usually less than a monolayer. The limited number of reactive surface sites [10,11] and the steric hindrances between bulky ligands in the chemisorptions layer [12,13] are the reasons.

2.2 Surface saturation and self-limiting reactions

Irreversible chemisorptions happen during the ALD cycle. In the gas-solid reaction of Step #1 and Step #3, atoms which are to be included in the ALD-grown film are adsorbed on the surface. Simultaneously, atoms which are not to be included in the ALD film may be removed as gaseous reaction by-products [1]. This is because the chemical bonds are formed in the interaction between the adsorbing molecule and the solid surface [14]. In addition, the adsorbed material may not be desorbed from the surface during the purge or evacuation.

After the adsorptions, the entire adsorption sites on the surface are occupied by the adsorbed species. The surface accepts only one layer, a monolayer, of the adsorbed species. Simply, the reactants take up the whole surface sites, and no further adsorption takes place after that. This is the surface saturation stage in ALD process.

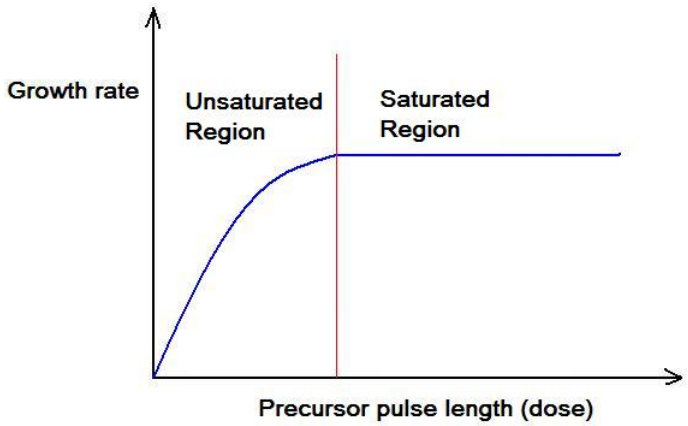

Figure 2 *Growth rate versus precursor pulse length (dose).*

For an ideal ALD process, under the conditions of irreversible chemisorptions and surface saturation, the precursor dose has no effect on the growth rate provided that the surface is saturated, i.e. all available surface sites are occupied by adsorbed precursor molecules (see ***Figure 2***). Therefore ALD film growth is a self-limiting process: the amount of the film material deposited during each cycle is constant [8]. In other published research, this process is also referred to as *self-terminating* [1] or *surface controlled* [4].

2.3 ALD window

The ALD temperature window is presented in Figure 3, which indicated the temperature range where thin film growth proceeds by the self-limiting reaction in an ALD mode [4]. Outside the ALD window, the growth is limited by precursor condensation (B), decomposition (D), and desorption (C) or by insufficient reactivity (A). Different lines and regions indicate the self- limiting growth related to the growth temperature and other aspects. Curve A expresses that the self-limitation is not reached because of the slow reactions; Curve B denotes that the self-limiting growth rate is exceeded because of the multilayer adsorption or condensation; Curve C figures that the self-limitation is

not maintained because of precursor desorption; Curve D expresses the self-limiting growth rate exceeded because of precursor decomposition.

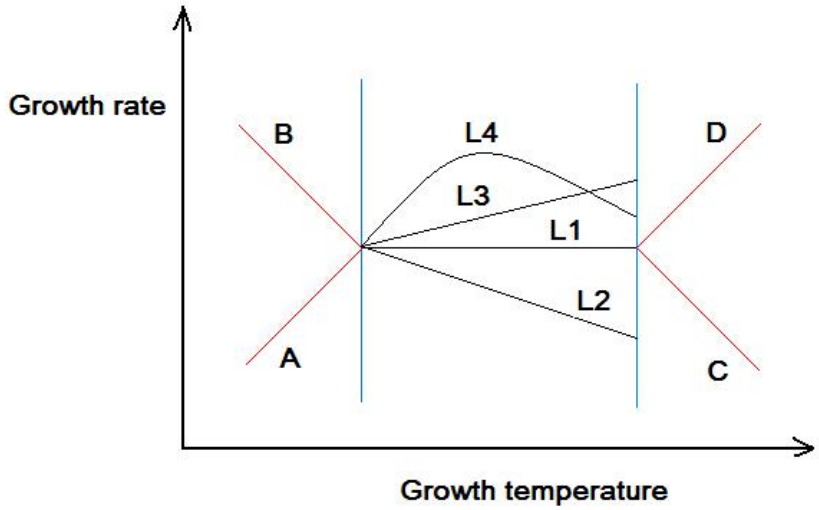

Figure 3 *ALD growth rate as a function of growth temperature (ALD window).*

In ***Figure 3***, the straight line L1 shows the self-limiting growth with temperature independent rate [15,16]. Nevertheless, this only occurs if steric hindrance causes saturation and the number of reactive sites does not change when the growth temperature is varied [17,18].

Usually precursors do not exhibit a distinct ALD window and thus the deposition rate in these processes is dependent on the temperature (see ***Figure 3*** L2, L3, L4). However, they can still be used for self-limiting ALD processes [4].

The straight line L2 express that the self-limiting growth decreases with temperature. The growth rate of all metal fluoride thin films decreased with increasing deposition temperature [19].The straight line L3 figures that the self-limiting growth increases with temperature. Curve L4 shows that the growth rate first increases and then decreases with temperature.

2.4 Advantages and limitations of ALD

The advantages of ALD can be divided into three aspects. Due to the feature of alternately pulsing and gas-solid reaction, there is no gas phase reaction. The precursors are highly reactive, thus enabling effective material utilization at low processing temperatures.

The self limiting feature contributes to the inherent advantages of ALD. Since each cycle deposits exactly the same amount of material, the film thickness can be accurately controlled simply by the number of deposition cycles. There is no need to control the reactant flux homogeneity over the substrate, if there is a large enough flux the chemisorptions will saturate. As a result, ALD provides good conformality and trench fill capability as well as good large area uniformity and large batch capability.

Finally the processing temperature windows are often wide, and the processing conditions of different materials are readily matched, giving ALD the capability to prepare multilayer structures in a continuous process. Low processing temperatures by suitable selection of the precursor chemistry is also possible.

The main limitation of ALD is the slowness since only less than a monolayer of film is deposited during one cycle. For some important materials, the lack of a working process also limits the application of ALD.

3 Precursor chemistry

Precursor chemistry is the key issue to a successful ALD process and also the first consideration for any new process. There are some general requirements for a suitable ALD precursor [4]:

- Sufficient volatility at the deposition temperature
- No self-decomposition allowed at the deposition temperature
- Precursors must react with the surface sites
- Sufficient reactivity towards the other precursor
- No etching of the substrate or the growing film
- Availability at a reasonable price
- Safe handling and preferably non-toxicity

The evaporating pressure of the precursor is an important parameter. The temperature will affect the precursor vapor pressure, which will influence the dose optimization together with pulsing length and methods. Due to various precursor states such as gas, solid and liquid, different pulsing methods should also be considered. Gas precursors are easy to pulse to the reactor. Liquid and solid precursor can be heated to achieve higher vapor pressure. If the vapor pressure is not possible to increase with raising temperature, different pulse method can be applied to improve the precursor dose.

It is widely accepted that in the ALD growth of oxide thin films, surface hydroxyl groups play an important role as intermediate species on the surface of the growing film after the water exposure [30]. During the subsequent metal precursor exposure sequence, the hydroxyl groups on the surface react with the incoming metal compounds.

$$x-OH+ML_n(g)\longrightarrow(-O-)_xML_{n-x}+xHL(g) \quad (1)$$

$$(-O-)_xML_{n-x}+\frac{(n-x)}{2}H_2O(g)\longrightarrow(-O-)_xM(-OH)_{n-x}+(n-x)HL(g) \quad (2)$$

where x – , M and L separately denote the surface, metal and ligand. The dehydroxylation increases with increasing temperature causing a gradual decrease of the surface hydroxyl group density. The amount of metal precursor anchored to the surface is determined either by the steric hindrances between the $(-O-)_xML_{n-x}$ surface species or by the density of the hydroxyl groups. Therefore, under conditions with extensive dehydroxylation, the hydroxyl group density may become a limiting factor in respect to the film growth rate.

In this work, trimethylaluminum (TMA), $TaCl_5$ (solid precursor) and H_2O (liquid precursor) are investigated to optimize the pulse length and method in their ALD processes.

The TMA and H_2O process is considered ideal for the Al_2O_3 growth process. The reactants are quite reactive while thermally stable, and the gaseous reaction product, methane, does not affect the deposition. This surface chemistry process is usually divided as two “half reactions” as presented in,

$$-Al-OH(s)+Al(CH_3)_3(g)\longrightarrow-Al-O-Al(CH_3)_2(s)+CH_4(g), \quad (3)$$

$$-Al-CH_3(s)+H_2O(g)\longrightarrow-Al-OH(s)+CH_4(g), \quad (4)$$

where the (s) and (g) represent surface groups and gas species respectively.

The chemical equation of the whole process is presented in,

$$Al(CH_3)_3(g) + \frac{3}{2}H_2O(g) \longrightarrow \frac{1}{2}Al_2O_3(g) + 3CH_4(g) \qquad (5)$$

Tantalum oxide thin films have been intensively studied because of their wide applications in different technology. The chemical equation is presented as,

$$2TaCl_5(g) + 5H_2O(g) \longrightarrow Ta_2O_5(s) + 10HCl(g) \ . \qquad (6)$$

After the H_2O pulse, the surface has an abundance of OH groups. The surface hydroxyls generally act as adsorption or reaction sites for the metal chloride. The hydroxyl groups are responsible during the adsorption of chlorides [20]. This surface chemistry mechanism could be also taken into account to explain the Ta_2O_5 growth as well as:

$$x - OH + TaCl_5(g) \longrightarrow (-O-)_x TaCl_{5-x}(s) + xHCl\,, \qquad (7)$$

when the surface is exposed to $TaCl_5$, the reaction releases HCl, which may react with the surface -OH groups or oxygen bridges,

$$(-OH)(s) + HCl(g) \longrightarrow (-Cl)(s) + H_2O(g)\,, \qquad (8)$$

$$(=O)(s) + HCl(g) \longrightarrow (-OH)(s) + (-Cl)(s)\,, \qquad (9)$$

$$(=O)(s) + 2HCl(g) \longrightarrow 2(-Cl)(s) + H_2O(g)\,. \qquad (10)$$

Thus, the adsorption sites can be occupied by the metal chloride or HCl, which can limit the concentration of adsorption sites or cause steric effects. On the other hand, the total area occupied limits the adsorption process. Steric effects must be considered when the

area occupied by an absorbed molecule or ion exceeds the area of one adsorption site. When a metal chloride is used as a precursor in ALD, the steric effects usually play an important role because the ionic radius of Cl^- significantly exceeds the size of the other ions or atoms participating in the reactions. In a simplified case, one can assume that the chemisorptions of the chloride stops when the surface concentration of Cl^- ions has attained a certain level. Moreover, the HCl released during the chloride pulse can react with the oxide surface. Chlorination of the surface by HCl as shown in (8)-(10) obviously hinders the adsorption of the metal chloride and reduces the growth rate [33].

4 ALD technology

The successful realization of ALD usually needs many different kinds of techniques, such as precursor, reactor, gas/liquid/solid sources controlling and delivering, cooling & heating, vacuum controlling and so on. In this section according to the optimization purpose of this work, five important aspects will be explained, which are precursor chemistry, ALD reactor, reaction chamber, precursor pulsing and valving, as well as precursor dosing technique.

4.1 ALD equipment

ALD equipment is the most important part in the whole ALD system. It includes a reaction chamber, a vacuum chamber, precursor cylinders, inert gas control, gas deliver lines, pulse valves, cooling and heating parts, as well as a vacuum pump. The reaction chamber and part of the lines and heaters are inserted into a vacuum chamber.

One challenge of ALD is the *throughput* in the ALD manufacturing of today. There is a requirement for cost effectiveness of the process for the exposure and purge sequences. The flow type ALD reactor has the ability to minimize the pulse and purge time and to maximize the precursor utilization efficiency. Therefore it is preferred in production and become the most common commercial ALD reactor. The flow type reactor is usually operated under viscous or transition flow conditions at pressures from 0.1 to 10 millibar

(1 millibar= 10^{-3} bar=10^{2} Pa). Inert gas is used for transporting the precursor vapors and purging the reactants. It can also be used as valving gas. The inert gas flow speed is usually high so that the gas mixing caused by diffusion is limited. This speed is regulated by a mass flow controller (MFC). In a research ALD device, the flow speed usually ranges from 100 to 1000 sccm (standard cubic centimeter per minute, 1000sccm =1 slm-standard liter per minute).

Plasma enhanced ALD (PEALD) is increasingly gaining interest. The plasma ions provides the required activation energy so that it can produce a better quality film at lower temperature than thermal ALD. This property is quite useful for temperature sensitive surfaces like on polymers. The ligands of the adsorbed precursor are removed with the plasma activated N_2, H_2, O_2, NH_3 species, which will affect the material properties. However, the PEALD reaction chamber is more complex with an additional plasma source and other issues.

4.2 Reactor

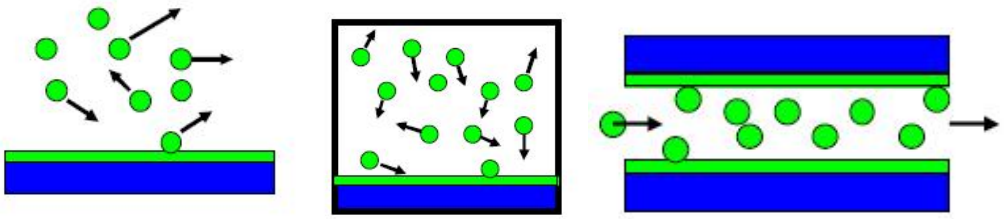

Figure 4 *Open chamber, closed chamber, and flow chamber.*

The reaction chamber is the place where the ALD reactions take place. There are three kinds of ALD chambers (***Figure 4***). An open chamber can incorporate any arbitrarily shaped substrate but with slow and poor efficiency. An closed chamber is good for high surface area，deep trench and porous materials but is slow for flat substrates, and there

may be also condensation problems. A flow chamber is fast and has good flow dynamics and high efficiency, therefore it is the mostly used ALD chamber.

There are different classified methods of ALD reactors. According to the precursor flow direction, there are *cross flow type reactor* (***Figure 5***) and *showerhead flow reactor*. With regards to the pressure in the reactor, there are *ultra high vacuum reactor* and *viscous or transition flow reactor*. According to activation energy applied, there is *thermal reactor* and *plasma enhanced reactor*. According to the number of wafers in the reactor, there is s*ingle wafer reactor* (***Figure 5***) and *batch reactor* (***Figure 6***).

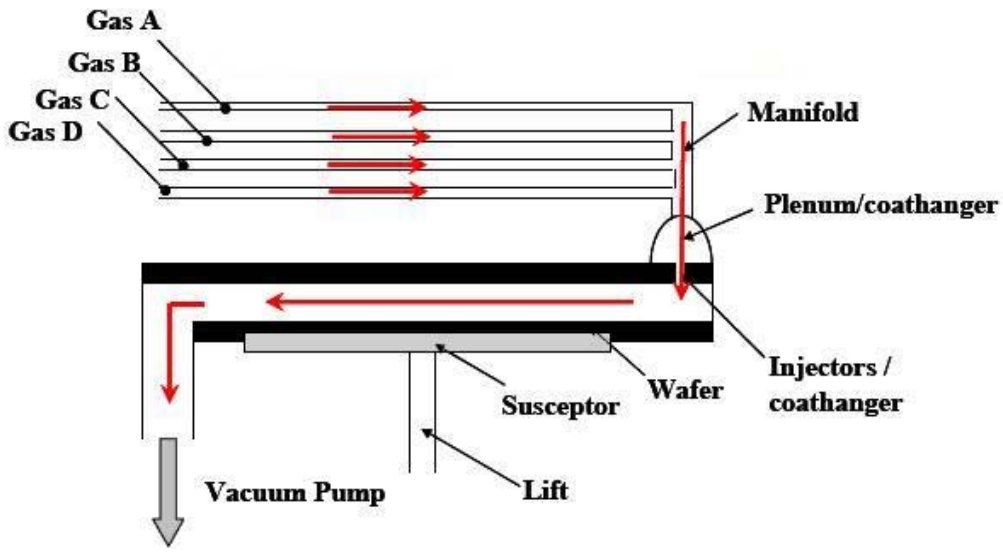

Figure 5 *Cross flow type ALD reactor [21].*

Figure 6 *Example of a batch reactor with thousand silver jewelleries being coated at one time (Copy right Beneq Oy, Finland).*

In the flow reactor, the precursor molecules are pulsed into the reaction chamber and transported by the carrier gas along the flow channel. The flow velocity and pressure are optimized to purge the reactants and separate the different precursor. The precursor will hit and collide with the substrate, and then find a chemisorptions site from front to substrate. Therefore, the front part of the substrate firstly receives the precursor molecules. The latter parts of the substrate will not receive any precursor molecules before the front parts are covered.

4.3 Precursor pulsing methods

In order to realize the alternately pulsing, there are usually precursor and transporting gas delivery lines and different valving methods applied in the precursor pulsing system. The kind of valve and method used depends on the vapor pressure of the precursor source.

For the high vapor pressure sources such as gases and high volatile liquid precursors, mechanical valves such as solenoid or pneumatic valves are usually used to pulse them from container into the reaction chamber. The container can be easily arranged outside of the reaction chamber. For a common flow type ALD reactor, the pressure of the reaction chamber is usually lower than the pressure of the precursor source. Therefore, the precursor can be transported into the reactor due to the difference of pressure. In addition, needle valves can be used for controlling the precursor dose.

For low vapor pressure precursor sources, pulsing is more complex. Usually there is requirement to heat the precursor far above room temperature to evaporate the solid precursor. When the required temperature is not too high, such as 100-300 ℃, the cylinder equipped with heating components can be used outside of the reaction chamber and the evaporated precursor can be pulsed with mechanical valves and transported to the reaction chamber by pressure difference or a transport gas. The optimization experiments conducted in this paper are exactly in this case. The detail of the valving and pulsing methods will be explained in **Section 7.2**.

If the evaporated temperature is too high for pneumatic valves, like 300-500 ℃, the solid precursor can be held by a source boat inside or very close to the reaction chamber. In this case, a mechanical valve is not possible to be used because it cannot endure such high temperatures. The precursor pulsing is controlled by inert gas valving.

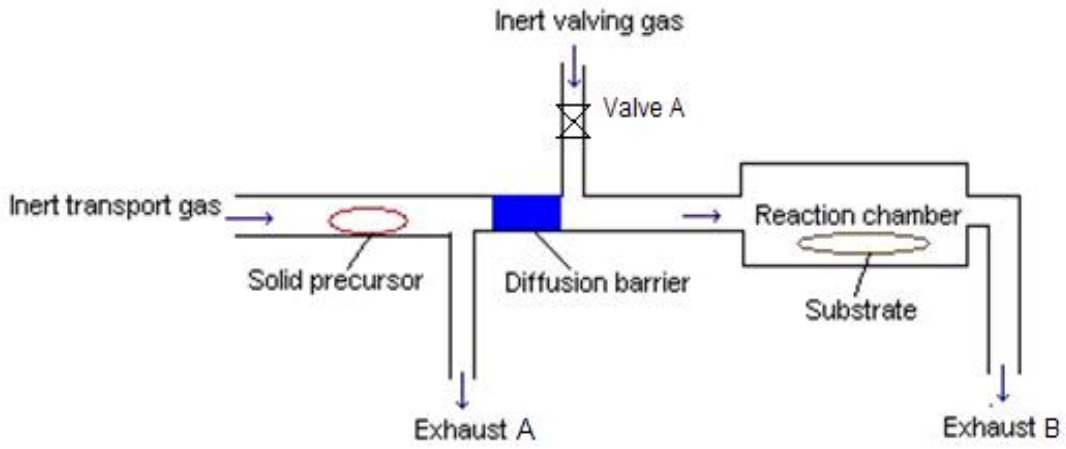

Figure 7 *A schematic of the inert gas valving.*

A schematic of the inert gas valving system is shown in ***Figure 7***. When the inert transport gas is closed, the valve A is open. The valving gas causes a diffusion barrier. The flow rate of the barrier gas is set to equal or greater than the rate of the precursor diffusion so that the precursor gas is hold up or switched off into the reaction chamber. When the inert transport is open, and the valve A is closed, the barrier will be broken down and the precursor can be transported into the reaction chamber. All the operation can be performed rapidly by the valves far away from the hot precursor.

4.4 Precursor dose

The precursor dose refers to the amount of precursor input into the reactor during ALD pulse. It depends on the precursor pulse length, the carrier gas flow rate, the precursor temperature and reactor pressure. In an ideal ALD reaction, the growth rate should saturate as a function of the precursor dose. The dose is a very important parameter which affects the film growth.

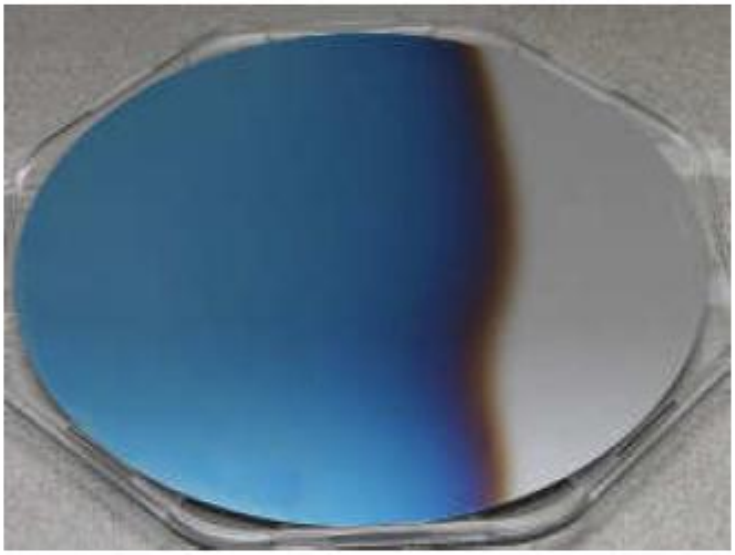

Figure 8 *An example of ALD film growth by underdose condition.*

Precursor pulse length is a common diversified parameter when the other parameters are constant. If the precursor pulse length is shorter than the saturation pulse length, an underdose will occurs. Under this condition, there are not enough precursor molecules to reach all of the active sites on the substrate. Therefore, the self-limiting growth mechanism cannot be satisfied. When one precursor is an underdose, it is easy to observe two distinct regions on the substrate as in ***Figure 8***.

In a non-ideal ALD process, there may be a chemical vapor deposition reaction (CVD) if the precursors are overdose and purge time is not long enough. Overdose will take place if the precursor pulse length is longer than the point after growth rate saturation. In addition, precursor decomposition must be avoided as this would also lead to a CVD type growth (see **Figure 9**).

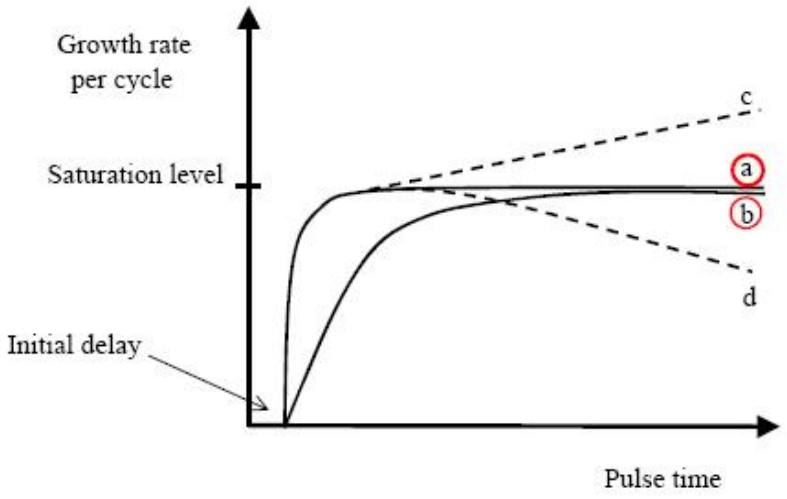

Figure 9 *(a) Fast chemisorptions reactions with no decomposition or etching; (b) slow chemisorptions reactions with no decomposition or etching; (c) chemisorption reactions followed by precursor decomposition; (d) chemisorption reactions followed by etching reactions[21].*

Thus, in order to avoid underdose and overdose occurring as mentioned above, it is very important to optimize the pulse length or other dose parameters of different precursors in ALD process. At the same time, the optimization of pulse length can also minimize the precursor pulse length and maximize the precursor utilization efficiency.

5 Modeling of precursor pulsing

In this part, the modeling of precursor pulsing with a solenoid valve from source cylinder to reaction chamber is presented.

5.1 Gas and low vapor pressure sources

Markku Ylilammi has reported a detailed model of pulsing through a solenoid valve, in which the pressure in the cylinder is assumed to be the same as the precursor vapor pressure in the equilibrium conditions P^* [12]. **Figure 10** shows a schematic illustration of the device. The parameters in the figure will be used in the calculation.

The transition of precursor from liquid to gas can be characterized by Clausius-Clapeyron's equation [22], where the vapor pressure of the precursor is a function of temperature,

$$\frac{d(\ln P^*)}{dT} = \frac{c_1}{T^2} \quad (1)$$

where c_1 is a constant for different precursor. The vapor pressure can also be found directly from chemical data books.

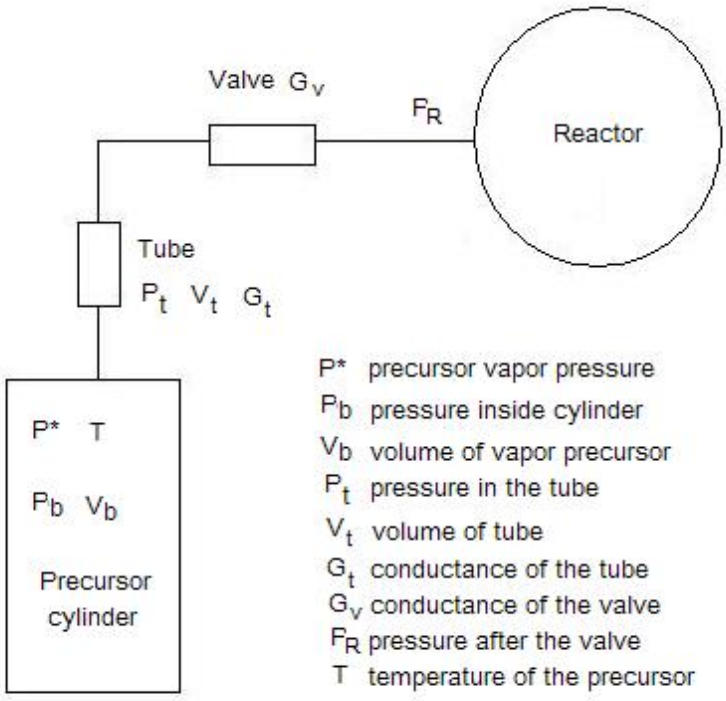

Figure 10 *Precursor pulsed by a solenoid valve from cylinder.*

The vapor pressure of the precursor should be higher than the pressure in the reaction chamber, otherwise there will be no flow from the precursor cylinder to the reactor. When the valve is opened, P_b is higher than P_R, which leads to the precursor flow from the cylinder to the tubes. The gas flow from the precursor cylinder to the reactor can be calculated by using Poiseulle's equation [23].

$$\frac{dn}{dt} = G_t \frac{P_b^2 - P_R^2}{\eta RT} \qquad (2)$$

where R is the gas constant, n is the amount of precursor, t is the time, η is the viscosity of the precursor and the conductance of the tube is G_t, which can be expressed by,

$$G_t = \frac{\pi d^2}{256L} \qquad (3)$$

where d is the diameter of the tube and L is the length of the tube.

The equation for the pressure P_t in the tube [12] is,

$$V_t \eta \frac{dP_t}{dt} = -(G_t + G_v)P_t^2 + G_s P^{*2} + G_v P_R^2 \quad (4)$$

The pressure after time t from the valve opening [12] is,

$$P_t = P_{ss} \frac{e^{t/\tau} + (P(0) - P_{ss})/(P(0) + P_{ss})}{e^{t/\tau} - (P(0) - P_{ss})/(P(0) + P_{ss})} \quad (5)$$

where the steady-state pressure and time constant are,

$$P_{ss} = \sqrt{\frac{G_s P^{*2} + G_v P_R^2}{G_s + G_v}} \quad (6)$$

$$\tau = \frac{\eta V}{2\sqrt{(G_s + G_v)(G_s P^{*2} + G_v P_R^2)}} \quad (7)$$

If the time constant τ is small compared to the pulse length, the result is valid for pressure gas cylinders or low vapor pressure sources. If the time constant is long compared to the cycle time, the pressure P_t can be assumed to remain at a steady-state value.

5.3 High vapor pressure sources

If the pulsed precursor has high vapor pressure in the cylinders (such as TMA, which has a vapor pressure at 20 ℃ of 1206 Pa), the pressure in the cylinder will change when the pulse valve is opened. The equations above (5), (6) and (7) are not satisfied under

this condition. An improved model will be shown below for high vapor pressure precursor pulsing through a solenoid valve from the source cylinder.

From the ideal gas equation,

$$\frac{PV}{T} = nR \qquad (8)$$

when the temperature T and volume V are constants, the gas equations can be differential as,

$$dn_t = \frac{V_t}{RT} dP_t \quad (9)$$

$$dn_b = \frac{V_b}{RT} dP_b \quad (10)$$

where dn_t and dn_b are the amount of vapor precursor in the tube and the container.

When the valve G_v is closed, the liquid precursor will evaporate continuously, and the partial pressure in the container (P_b) will increase. Then P_b will be higher than the pressure before the valve (P_t). Due to the pressure difference, the precursor vapor will flow from the container to the tube until the saturation state ($P_b = P_t$) is achieved. The process can be calculated by using equation (2).

$$\frac{dn_t}{dt} = G_t \frac{P_b^2 - P_t^2}{\eta RT} \quad (11)$$

By using equation (9) we get,

$$\frac{dP_t}{dt} = G_t \frac{P_b^2 - P_t^2}{\eta V_t} \quad (12).$$

Because the amount of vapor precursor is equal to the sum amount of vapor precursor in the tube and the container,

$$dn = dn_b + dn_t \quad (13),$$

Substitution (9) and(10), then

$$\frac{dn}{dt} = \frac{V_b}{RT}\frac{dP_b}{dt} + \frac{V_t}{RT}\frac{dP_t}{dt} \quad (14)$$

The evaporation of the liquid precursor in the container can be expressed by Langmuir's equation [24],

$$\frac{dn}{dt} = \frac{P^* - P_b}{\sqrt{2\pi MRT}} cA \quad (15)$$

where M is the molar mass of the precursor, A is the area of the vaporizing surface, and c is a vaporization constant.

From (12), (14) and (15), dP_b can be expressed as follows:

$$\frac{dP_b}{dt} = \frac{P^* - P_b}{\sqrt{2\pi MRT}} \frac{cATR}{V_b} - G_t \frac{P_b^2 - P_t^2}{\eta V_b} \quad (16)$$

When the valve G_V is opened after the saturating state ($P_b = P_t > P_R$), P_t is higher than the pressure behind the valve P_R. Because the reactor and tube behind the valve has been evacuated during the purge step and the volume of the reactor is much larger, the V_b and V_t, P_R can be assumed to remain as a constant. Due to the pressure difference, the

vapor precursor will flow through the valve until the steady state ($P_b = P_t = P_R$), and P_b and P_t will decrease until reaching a steady state.

The flow rate of the precursor through the valve can be calculated by using equation (2),

$$\frac{dn_R}{dt} = G_v \frac{P_t^2 - P_R^2}{\eta RT} \quad (17).$$

By using the eqution (15), (16) and (17) for the process of the valve from open to close, the equation of the pressure in the cylinder and tube can be calculated by using the following differential equation group:

$$\frac{dP_b}{dt} = \frac{P^* - P_b}{\sqrt{2\pi MRT}} \frac{cATR}{V_b} - G_t \frac{P_b^2 - P_t^2}{\eta V_b} \quad (18)$$

$$\frac{dP_t}{dt} = G_t \frac{P_b^2 - P_t^2}{\eta V_t} - G_v \frac{P_t^2 - P_R^2}{\eta V_b} \quad (19)$$

6 Ellipsometry

Ellipsometry is an optical measurement technique based on polarized light reflection from samples and has been widely applied to evaluate thin film thickness and uniformity. One of the remarkable features of spectroscopic ellipsometry is the precision of the measurement. Moreover, the feature of nondestructive and fast measurement within only a few seconds contributes it to be used in wide application area. ***Figure 11*** shows an optical model represented by the complex refractive index and layer thickness of each layer. Parameters of n_0, n_1 and n_2 denote the complex refractive indices of substrate, air and thin film, respectively.

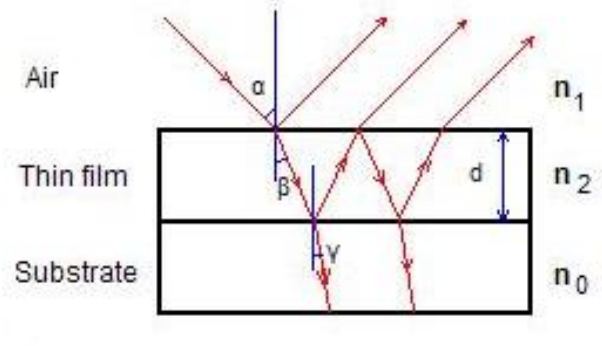

Figure 11 *Optical model consisting of an air / thin film / substrate structure*

The key feature of ellipsometry is measuring the change in polarized light upon light reflection from a sample. The amplitude ration Ψ and phase difference Δ between

light waves known as p- and s-polarized light are measured. In ellipsometry the variation of light reflection with p- and s-polarizations is measured as the change in polarization state. In particular, when the sample structure is simple, the amplitude ratio is characterized by the refractive index n, while phase difference represents light absorption described by the extinction coefficient k. In this case, the two values (n, k) can be determined directly from the two ellipsometry parameters (Ψ , Δ) obtained from a measurement by applying the Fresnel equations. This is the basic principle of ellipsometry measurement.

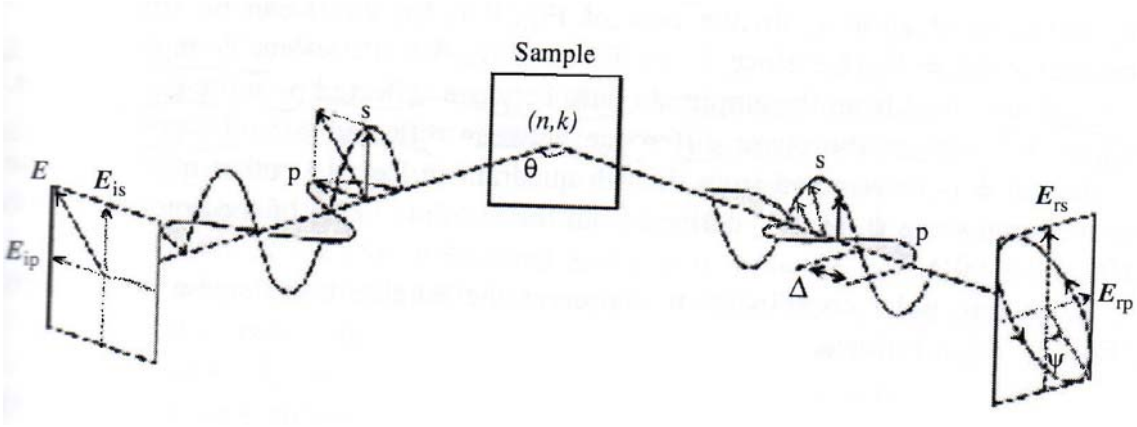

Figure 12 *Measurement principle of ellipsometry [25].*

The measured angles of (Ψ , Δ) from ellipsometry are defined from the ratio of the amplitude reflection coefficients for p- and s-polarizations (see ***Figure 12***) [25]:

$$\rho = \tan\psi \exp(i\Delta) = \frac{r_p}{r_s} \qquad (1)$$

where the amplitude reflection coefficients for p- and s-polarized light are,

$$r_p = \frac{E_{rp}}{E_{ip}} = \frac{n_2 \cos\alpha - n_1 \cos\beta}{n_2 \cos\alpha + n_1 \cos\beta} \qquad (2)$$

$$r_s = \frac{E_{rs}}{E_{is}} = \frac{n_1 \cos\alpha - n_2 \cos\beta}{n_1 \cos\alpha + n_2 \cos\beta} \quad (3)$$

The transmission angles β and γ can be calculated from the angle of incidence α by applying Snell's law,

$$\frac{\sin\alpha}{\sin\beta} = \frac{n_2}{n_1} \quad (4)$$

$$\frac{\sin\beta}{\sin\gamma} = \frac{n_0}{n_2} \quad (5)$$

For transparent films, the film-thickness period *d* [26] in optical interference is expressed by

$$d = \frac{\lambda}{2n_1 \cos\beta} \quad (6)$$

In particular, when λ is fixed for reflectance measurements at normal incidence, the condition becomes $n_1 d = constant$, where the *nd* product is the generally called the optical thickness [25].

7 Experimental methods

7.1 Equipments at Micronova

The film growth were carried by using Beneq TFS-500 system in the Micronova cleanroom. This thin film system is designed for ALD research and production purposes. Substrate alternatives include wafers and other planar substrates, powders and porous substrates, as well as complex 3-dimensional substrates. There is a water cooled vacuum chamber wall and cross flow type reaction chamber in the system. Ultra high purity nitrogen (99.9999%) is supplied as the carrier and purge gas.

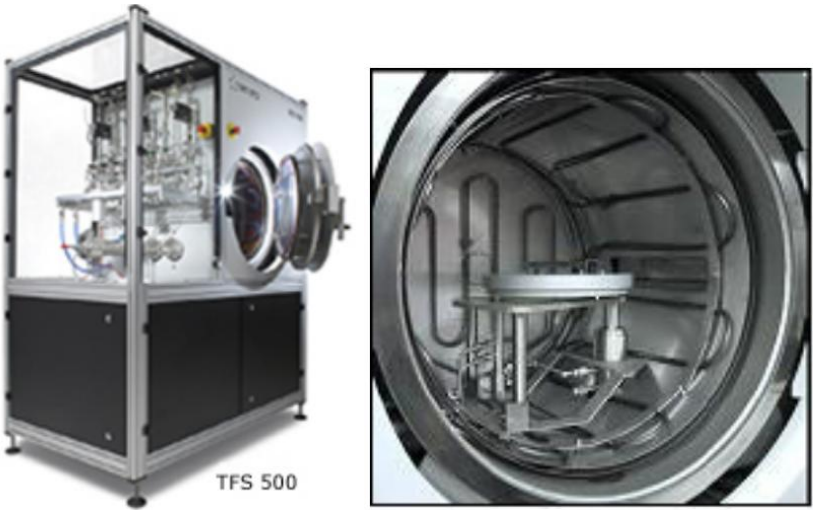

Figure 13 *TFS-500 ALD reactor and reaction chamber (Copy right Beneq Oy, Finland).*

Precursor cylinder of HS-200 installed in TFS-500 is designed for both liquid and solid precursors. It can be heated up to 200 °C in an oven-like heater. There are two ports with valves on the top of the cylinder. Different kinds of pulse methods can be applied so that the precursor can be pulsed effectively. The body is divided into two parts which are connected by 16 screws and a copper seal.

The sample was loaded and unloaded to the ALD reactor in a class of 1000 clean room environment. This clean environment can reduce particulate contamination of the samples. A UV lamp was used to detect the particles on the wafer before putting them into the ALD reactor, so that the film growth was not affected by the particles. Furthermore, most of the particles can be blown by N_2. In order to save wafer usage, a 8-inch silicon wafer was cut into 3 parts, which is sufficient for the optimization process (see ***Figure 14***).

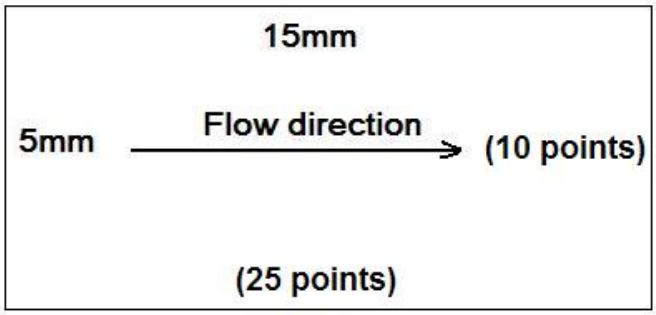

Figure 14 *Silicon wafer and flow direction*

The thickness and uniformity measurements were carried by the LASMOS SD 2300 ellipsometer in the cleanroom. It works using the rotating analyzer method and can be used for the measurement of film thickness and uniformity, as well as the refractive index of optically transparent and absorbing layers. The light source was a He-Ne laser with a wavelength of 632.8 nm. The time of measurement was under 1 s/point and the wafer size was up to 145 mm. The incidence angle range was from 35 ° to 73 °. Around

200 points are orderly chosen and measured on each piece of wafer. The thickness data was handled by Matlab software and the figures of thickness & uniformity mapping were finally gained.

Figure 15 *LASMOS SD 2300 ellipsometer [27]*

7.2 ALD pulsing modes

In order to efficiently pulse precursor into the reaction chamber, different kinds of ALD pulsing modes are designed according to the vapor pressure of various precursor. Carrier gas, such as N_2, can be used to take and blow the precursor out off the cylinder and into the reaction chamber if the vapor pressure of a precursor is low. **Figure 16** shows a schematic of the gas valve, reaction chamber and precursor cylinder. The Orifice is used to limit the N_2 flow rate. This unique design can create different kinds of pulsing modes by alternately opening valve A, B and C. In this section, four pulsing modes are introduced.

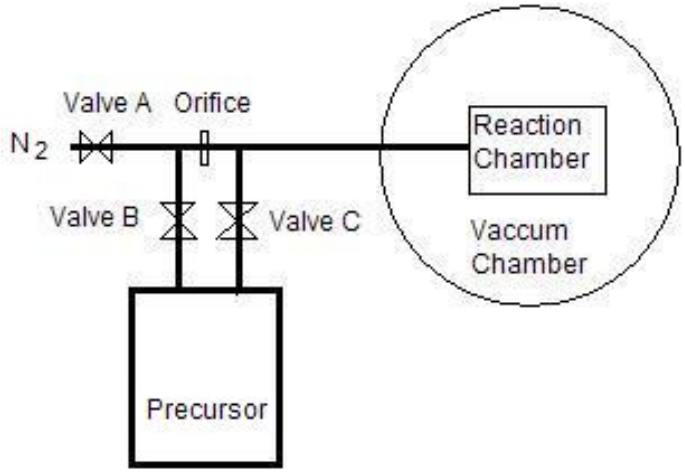

Figure 16 *A schematic of the valve, reaction chamber and precursor cylinder.*

7.2.1 Standard pulse mode

When the valve C (see ***Figure 16***) is open, high vapor pressure liquid precursors can be easily pulsed into the reaction chamber, which is referred to standard pulse mode. Except for TMA pulsing, $TaCl_5$ as a low vapor pressure solid precursor is validated again by standard pulsing mode.

7.2.2 Assistant flow pulse mode

Assistant flow pulse mode means firstly opening valve A, then opening valve C for a certain length of time and closing valve C, and finally closing valve A.

7.2.3 Overflow pulse mode

Overflow pulse mode means simultaneously opening valve A, B and C for a certain length of time. When valves are opened, the N_2 carrier gas flows through the chamber to the reactor.

7.2.4 Booster pulse mode

Booster pulse mode means opening valves A and B for a certain while, and closing valves A and B, then open C. When both valves A and B are opened at the same time, the N_2 flow increases the pressure in the cylinder. This operation will help the precursor to be pulsed out when valve C is open.

7.2.5 Combination pulse mode

The combination pulse mode is an integration of booster pulsing and overflow pulsing mode. In great detail, the valves were pulsed the following sequence of operation: open valve A and valve B, close valve A and B, then open valve C for a length of time and close valve C, and then open valves A, B and C simultaneously.

8 Results and discussion

8.1 Simulation results of TMA pulsing

According to the modeling results in **section 5**, the simulation of TMA pulsing were carried out by Matlab software for the TMA pulsing. The solver of ODE45 was used to plot P_t and P_b. The parameters are shown in Table 1. The parameters 7-15 are estimated values, according to the components in Beneq TFS-500 ALD reactor. The conductance of the valve is estimated according to the value of tube conductance. The pressure after the valve is assumed to be the pressure of the reaction chamber, which is measured by pressure sensor in the reactor. In the real case, there is carrier gas N_2 flowing through the point after valve, the partial pressure of N_2 effects this pressure. Therefore, the simulation result does not coincide with the real pulsing process very well.

The simulation results of TMA pulsing are shown in

Figure 17, the pressure in the cylinder does not change very much. This is probably because the vapor pressure is high, although there are precursor pulsed into the reaction chamber, enough precursors evaporate from liquid state again and increase the pressure within very short time. However, the pressure in the tube will decrease to a steady state if the pulsing length (open time) is long enough (more than 6 s). The steady pressure is

much higher than P_R so that the precursor can flow from the cylinder to the reaction chamber continuously. When the valve is closed, the pressure in the tube will increase and saturate again if the recovery time is long enough (more than 6 s). Here the recovery time depends on the length of the purge and the other precursor pulsing time. For porous material substrates, even though the pulse length is quite longer (100 s) than the normal millisecond level on flat substrates, the precursor molecules can penetrate into the deep holes due to the high pressure difference between the cylinder and reaction chamber.

Table 1 *Parameters of TMA pulsing simulation.*

1	TMA temperature	T=293K
2	Ideal gas constant	R=8.3145 J/mol*K
3	Viscosity of TMA	η=1.12 at 293K [28]
4	TMA molar mass	M=72 g/mol [28]
5	TMA vapor pressure	P^*=1206 Pa at 293K [28]
6	Vaporization constant	c=0.01 [29]
7	Radius of cylinder	r=0.025 m
8	Height of cylinder	h=0.1m
9	Area of TMA surface	A=0.0079m^2
10	Volume of vapor TMA	V_b=7.854*$10^{-4}m^3$
11	Diameter of the tube	d=0.006m
12	Tube length before valve	L=0.04m
13	Tube volume before valve	V_t=1.2566*$10^{-4}m^3$
14	Tube conductance	G_t=3.1416*10^{-7}
15	Valve conductance	G_v=0.5*10^{-10}
16	Pressure after valve	P_R=229 Pa

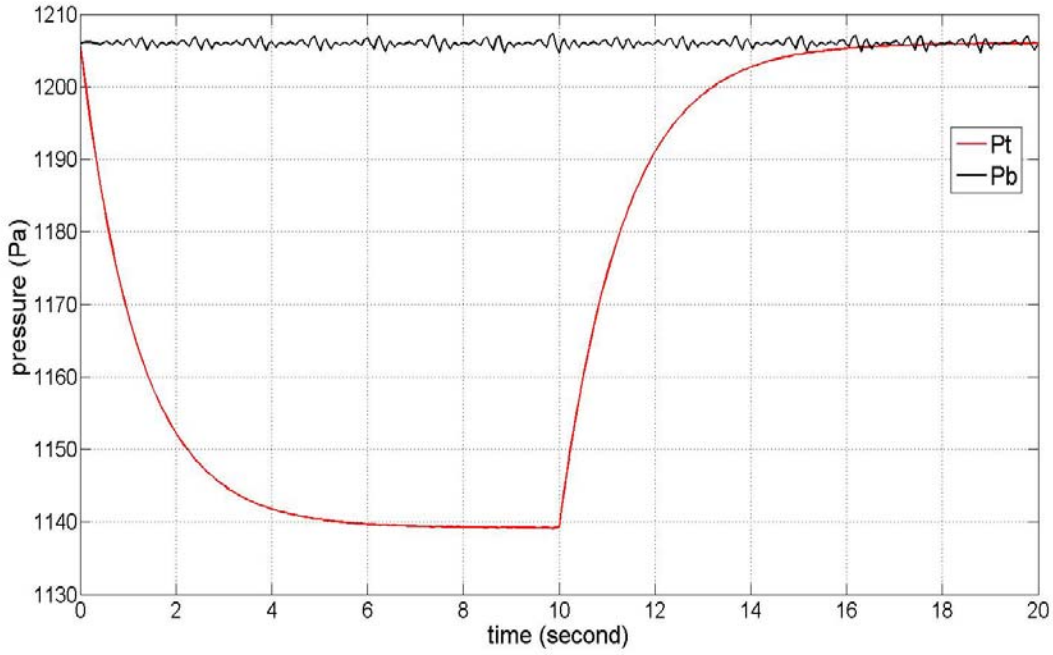

Figure 17 *TMA pulsing simulation results through a solenoid valve from cylinder.*

8.2 H_2O pulsing length optimization with TMA

In the optimization experiment of the new Beneq HS200 hot source, H_2O were used as the liquid source. TMA is used as the metal source in a normal liquid cylinder. The reactant sources were circularly injected into the reaction chamber in the following order: TMA vapor pulse 200 ms, N_2 gas purge 1 s, H_2O gas pulse and N_2 gas purge 1 s. The H_2O and TMA were kept at 20℃ and pulsed by the standard pulse mode. The reaction chamber temperature was 220℃. The pressure in the vacuum chamber and reaction chamber were 6.0 and 1.0 mbar separately. The flow rate of N_2 was 200 sccm and 1000 cycles was processed. Following pulse length of H_2O was used: 100 ms, 200 ms and 300 ms.

Table 2 *Comparison of measurement results at different H_2O pulse lengths.*

Al2O3	pulse length	thickness variations	mean thickness	growth rate
1	100 ms	0.441%	122.9 nm	1.23Å/cycle
2	200 ms	1.601%	129.2 nm	1.29Å/cycle
3	300 ms	14.144%	156.3 nm	1.56Å/cycle

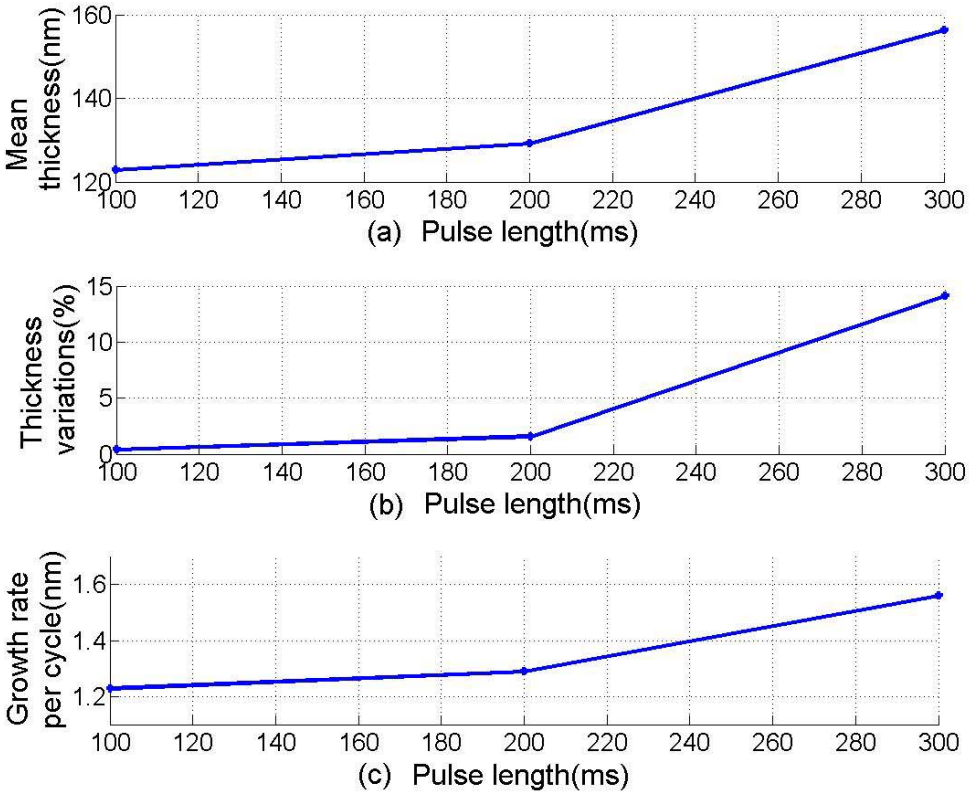

Figure 18 *H_2O pulse length versus film thickness (a), thickness variations (b) and growth rate (c).*

The ellipsometer results of Al_2O_3 film grown onto Si with different H_2O pulse length are shown in **Table 2** and ***Figure 18***. From ***Figure 18*** (c), although the pulse length is doubled, the growth rates of 100ms and 200 ms H_2O pulse lengths are only changed

from 1.23 Å/cycle to 1.29 Å/cycle. This small increase can be explained by the fact that the growth rate could be enhanced by increasing the water dose, which is believed to be due to the increased density of hydroxyl groups remaining on the film surface after the water pulse [30]. The growth rate is comparable to that of 1.2 Å/cycle under different experimental conditions [30]. The uniformity of the film with 100 ms pulse length is 0.441% and comparable to that of the TMA and water ALD process in other publications [1]. This behavior indicates that the optimized self-limiting ALD reaction is reached at a 100 ms or shorter pulse length. In an optimized self-limiting ALD process, a constant growth rate per cycle is achieved without additional film growth for prolonged source exposures. The close to constant growth rate implies that the self-limiting ALD process is proper without a CVD effect at a suitable substrate temperature for the pulse length around 100 ms [31].

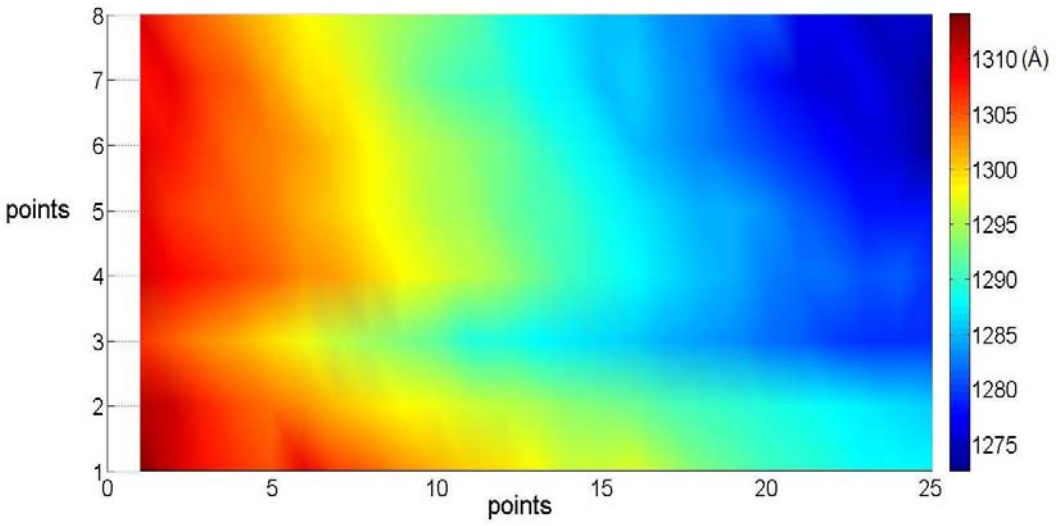

Figure 19 *Mapping of Al_2O_3 thickness at 100 ms H_2O pulse with good film.*

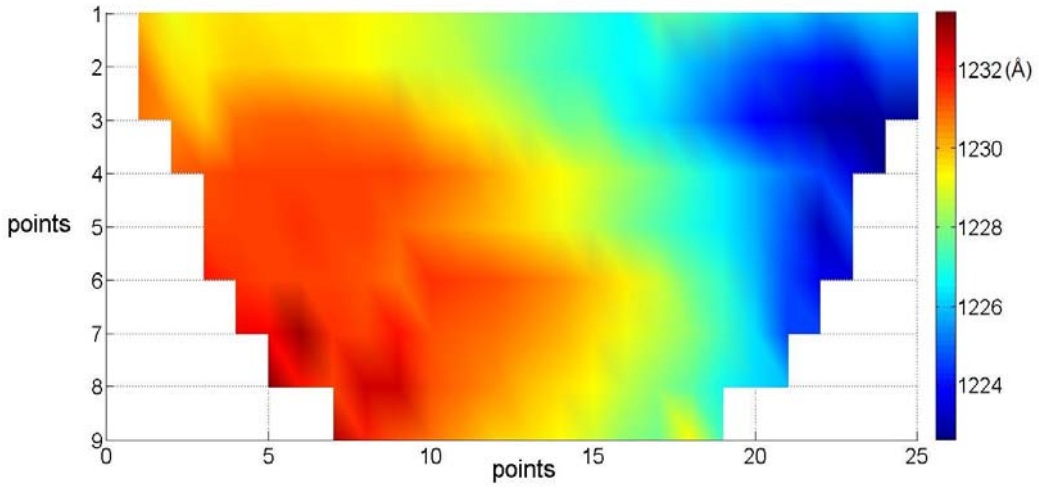

Figure 20 *Mapping of Al_2O_3 thickness at 200 ms H_2O pulse with good film.*

The thickness profiles of films are shown in the mapping of ***Figure 19*** and ***Figure 20***. The uniformity of the film with 100 ms H_2O pulse is 0.441% and better than 1.601% at 200 ms. The mean thickness difference is only 0.6 nm. At 200 ms, the different between the maximum thickness and minimum thickness is 0.4 nm. At 100 ms, the difference is 0.1 nm.

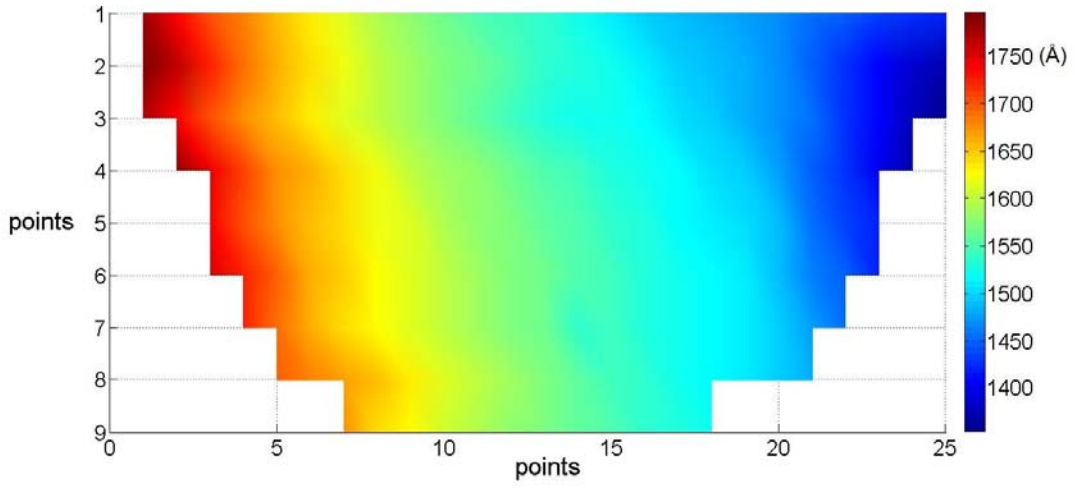

Figure 21 *Mapping of Al_2O_3 thickness at 300 ms H_2O pulse with over dose and CVD reaction.*

When the pulse length is 300 ms, the thickness variation of the film is about 14%. The mean film thickness increases to 156.3 nm. **Figure 21** shows the thickness mapping handled by Matlab software. The film at the front edge of the wafer is much thicker than that at the end edge. According the theory in Section 4.3.1, the non uniform film is caused by H_2O overdose. The purge time after the water pulse is still 1s and it cannot completely purge all the residual water vapor left in the reaction chamber. Therefore there is a CVD type of growth to be observed at the surface of the wafer.

8.3 The optimization of $TaCl_5$ pulsing length

In this experiment, $TaCl_5$ was used as the tantalum source and H_2O as the oxygen source. In order to find out the evaporation temperature of $TaCl_5$ in the precursor cylinder firstly, the combination pulse method including booster pulsing, standard pulsing, and overflow pulsing was applied sequentially. There were together 500 cycles for each experiment. The temperature started from 90 ℃ and increased 10 ℃ at a time. N_2 gas flow rate was 200 sccm. The temperature of reaction chamber was 200 ℃. H_2O pulse length was 200 ms. The purge time for both precursors was 2 s. The pressure in vacuum chamber and reaction chamber were around 6.00 and 1.00 mbar respectively. There was no film on the substrate when the temperature of the container is from 90 ℃ to 150 ℃. This indicates that the $TaCl_5$ precursor evaporation rate is sufficient when the cylinder temperature is 160℃ or higher.

In the pulse length optimization experiment, except that the $TaCl_5$ pulse time was changed as 500 ms, 250 ms, 100 ms, 25 ms, while the $TaCl_5$ cylinder temperature was still at 160℃, the pulse combination method and other parameters were kept the same as above experiment. The ellipsometer results of Ta_2O_5 film grown onto Si with different H_2O pulse length are shown in ***Table 3*** and ***Figure 22***.

Table 3 *Comparison of measurement results at different $TaCl_5$ pulse length*

Ta2O5	pulse length	thickness variations	mean thickness	growth rate
1	25 ms	4.645%	40.3 nm	0.81 Å /cycle
2	100 ms	5.668%	41.6 nm	0.83 Å/cycle
3	250 ms	11.39%	45.1 nm	0.90 Å/cycle
4	500 ms	4.781%	42.6 nm	0.85 Å/cycle

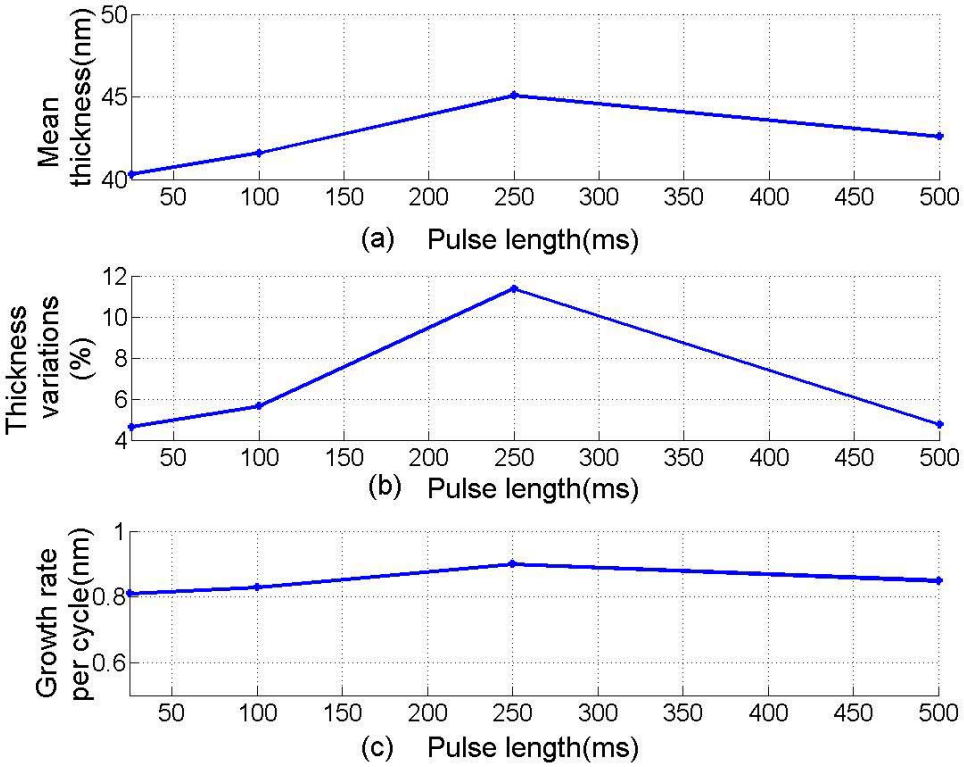

Figure 22 *$TaCl_5$ pulse length versus mean thickness, thickness variations and growth rate*

In Ta_2O_5 process, longer $TaCl_5$ pulse will lead to etching reactions, which is expectedly responsible for the decrease in growth rate and resulting thinner films [32].

Figure 22 (a) and (c) show that the mean thickness and growth rates do not decrease with the increment in $TaCl_5$ pulse length from 25 ms to 100 ms. It indicates that no marked etching effect occurs on the films. There is also no remarkable increasing for

the growth rate of samples with 25 ms and 100 ms pulse length, and they are almost at the same level of 0.8 Å/cycle that is comparable to the result for ALD reaction in ref. [33]. Therefore the self-limiting ALD process can be identified by the measurements of film thickness and growth rate against the H_2O pulse length at 25 ms and 100 ms.

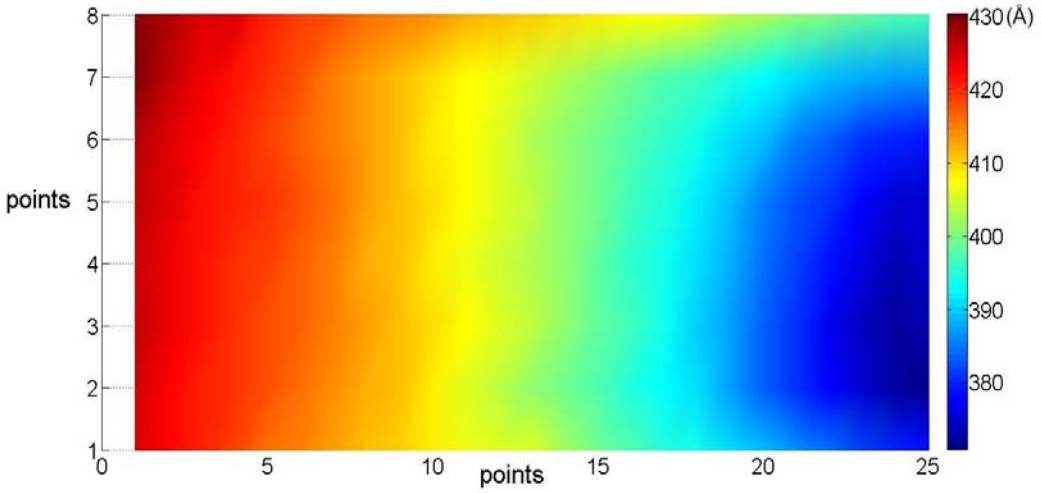

Figure 23 *Mapping of Ta_2O_5 thickness at 25 ms $TaCl_5$ pulse*

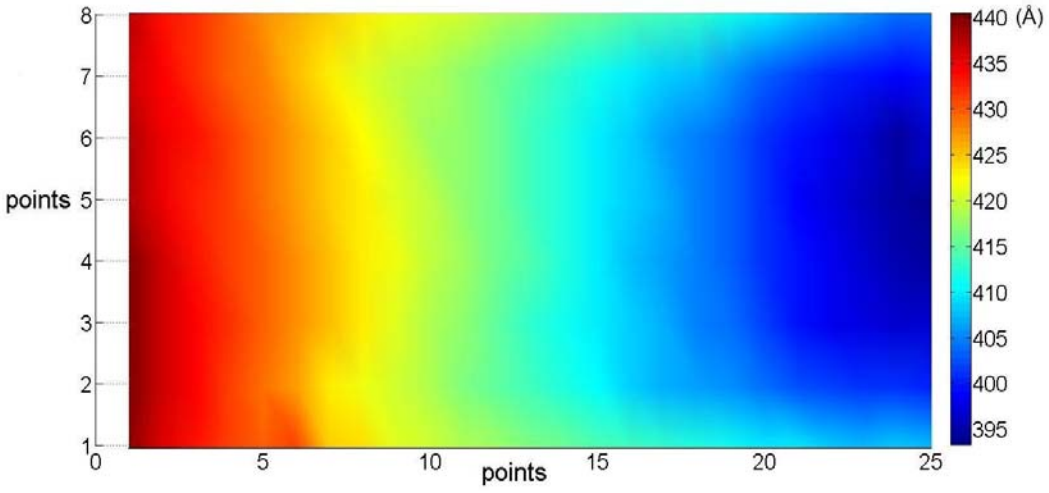

Figure 24 *Mapping of Ta_2O_5 thickness at 100 ms $TaCl_5$ pulse*

From ***Table 3***, the thickness variation of the two samples with 25 ms and 100 ms pulse are 4.6% and 5.7% respectively. The mapping of thickness profiles are shown in Figure 23 and Figure 24 for different pulse time. Three different regions from up to down can be seen in the flow direction. The thickness of ALD film usually decreases with increasing distance from the reactor inlet. Chemical vapor deposition have been suggested to be the cause of this phenomenon [34]. In ALD, direct intermixing of the precursors is avoided by purging the reactor with pure carrier gas between the precursor pulses. Nevertheless, in addition to chemisorptions, some amount of precursors can be physisorbed onto solid surfaces, most probably at the reactor inlet where the precursor concentration is highest. Desorption of the physisorbed precursor at the beginning of the next pulse results in mixing of precursors and CVD type growth. The latter mainly contributes to these additional films growth at the leading edge of the substrate.

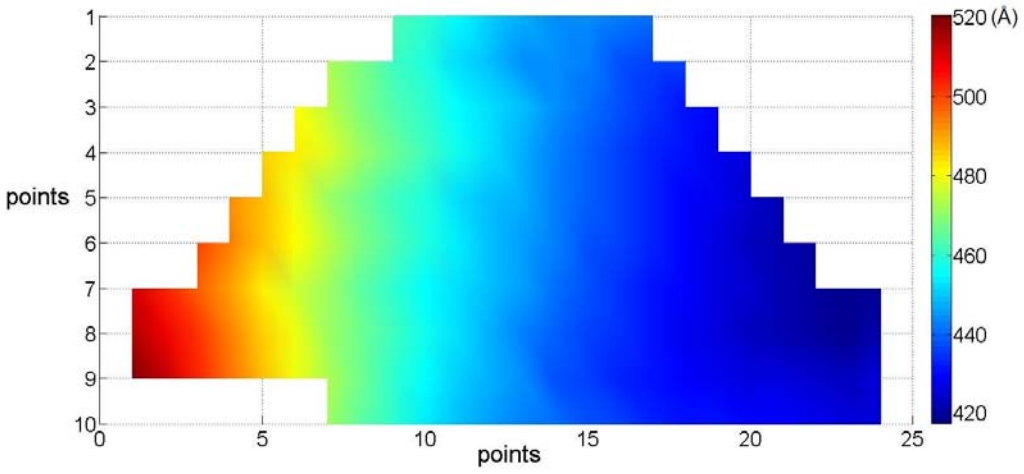

Figure 25 *Mapping of Ta_2O_5 thickness at 250 ms $TaCl_5$ pulse*

When the $TaCl_5$ pulse length is increased to 250 ms, the film uniformity rises quickly to 11.4%. The mean film thickness increases about 4 nm and up to 45.1 nm. Thickness profiles of films are showed in mapping ***Figure 25***. The growth rate reaches 0.90 Å/cycle. This phenomenon is contributed by the CVD reaction due to the short purge

time. During long enough purge periods, the reaction by products are desorbed and exhausted to minimize the concentration of residues. The reaction and nucleation in gas phase are thereby prevented. If the precursor dose is high, longer purge time is usually required. In this experiment, purge time was kept as a constant of 1 s, which lead to the gas phase reaction between residual and new precursor. Owing to the by-product residues, there should be also etching reaction between HCl and films, which is more obvious in 500 ms pulse $TaCl_5$ and will be illuminated detailed later. The increasing thickness and growth rate could be explained that the etching rate is still much lower than the film growth rate.

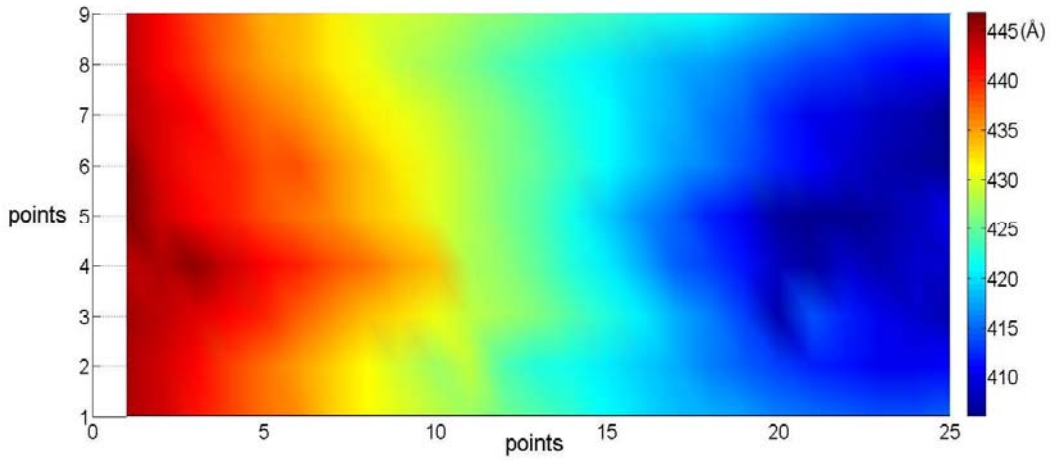

Figure 26 *Mapping of Ta_2O_5 thickness at 500 ms $TaCl_5$ pulse*

When the $TaCl_5$ pulse length is increased to 500 ms, the film uniformity redrops to 4.8%. Thickness profiles of films are showed in ***Figure 25***. The mean film thickness decreases to 42.6 nm. The growth rate falls to 0.85 Å/cycle. The reason for this thickness profile as well as mean thickness and growth rate descending could be secondary reactions between chemisorptions reaction products and the solid surface. Although there could be gas phase CVD reaction which is the same as in samples of 250 ms $TaCl_5$ pulse length, owing to the re-adsorption of reaction products, some

adsorption sites for the precursor are occupied and the growth rate should decrease, predominantly at the trailing edge of the substrate. In ALD of oxides from metal chlorides and H_2O, HCl is produced in the chemisorption reaction. HCl, which is released during the chloride pulse, can react with the oxide surface. Chlorination of the surface by HCl obviously hinders adsorption of the metal chloride and reduces the growth rate.

8.4 $TaCl_5$ pulse mode optimization

Although the combination mode has produced good quality film, there is still possibility to optimize the long pulse time and complex operation for each cycle. In order to improve the efficiency of total reaction time, optimal experiments of different pulse mode are carried out in this section.

8.4.1 Standard and assistant flow pulse mode

When applied to $TaCl_5$, the process parameters are the same as used in section 8.3. There was no film when the standard pulse or assistant flow pulse mode were used. The reason is that the pressure in the cylinder is too low to pulse enough precursors into the reaction chamber. Hence, for low vapor pressure sources, only when the pressure in the cylinder is higher than the pressure in the reaction chamber, the precursor can be pulsed through the valve C.

8.4.2 Booster pulse mode

In order to compare the results of combination mode, the booster pulse mode is carried out. The details processes are open valve A and B, close valve A and B, open valve C for 500 ms and close valve C. The other parameters are the same in section 8.3. The

measurement results are showed in ***Table 4***. ***Figure 27*** shows the film thickness mapping.

Table 4 *Measurement results comparison for $TaCl_5$ pulse mode optimization*

Pulse method	pulse length	thickness variations	mean thickness	growth rate
Combination	500 ms	4.781%	42.6 nm	0.85 Å/cycle
Booster pulse	500 ms	6.589%	40.4 nm	0.81 Å/cycle

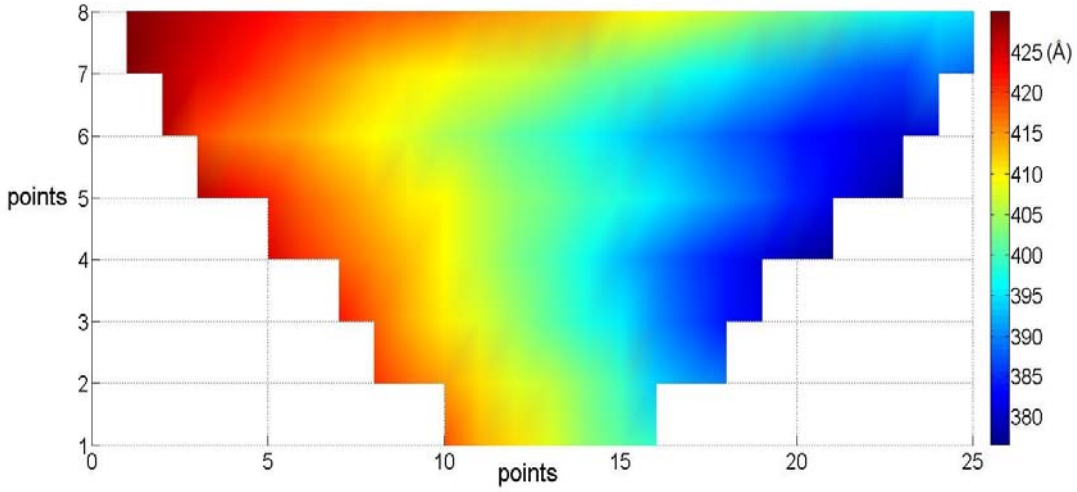

Figure 27 *Mapping of Ta_2O_5 thickness at 250 ms booster pulse mode*

There is no marked change between mappings of **Figure 26** and **Figure 27**. It can be seen from **Table 4** that the growth rate and the thickness of film grown by booster pulse mode are smaller than the film grown by combination mode. These indicate that different pulse mode could change the precursor dose.

8.4.3 Overflow pulse mode

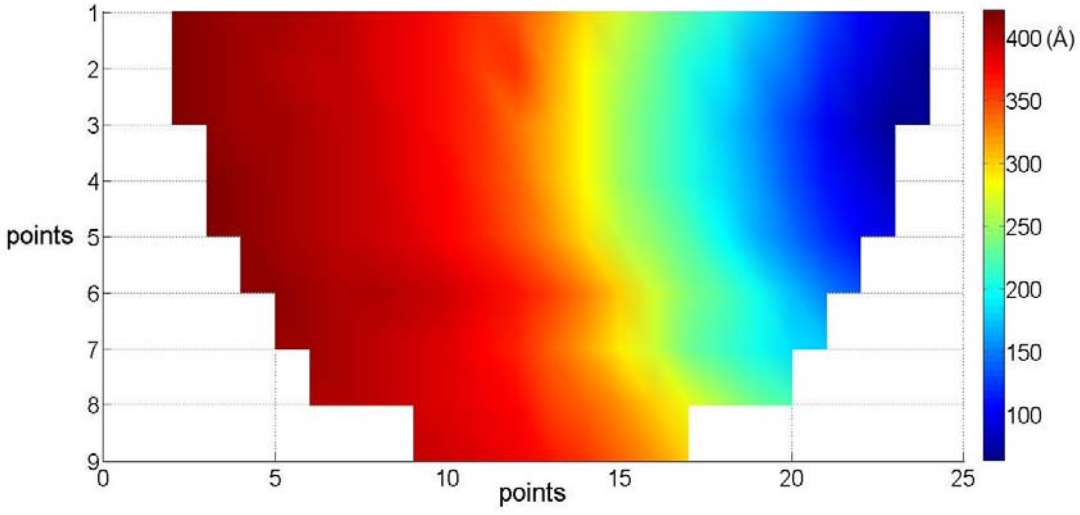

Figure 28 *Ta_2O_5 film grown by using 25 ms $TaCl_5$ overflow pulse mode*

Table 5 *Ellipsometry results of Ta_2O_5 film with combination and overflow pulse modes*

Pulse method	pulse length	thickness variations	mean thickness	growth rate
Combination	25ms	7.372%	40.3 nm	0.81 Å /cycle
Overflow	25ms	60.294%	29.6 nm	0.59 Å /cycle

The ellipsometry results of Ta_2O_5 film grown by using combination and overflow pulse modes are shown in **Table 5**. Low growth rate, small mean thickness and poor uniformity indicate that overflow mode does notpulse sufficient precursor effectively and the precursor underdose occurs. **Figure 28** shows the thickness mapping of the sample grown by overflow pulse mode. There are clearly different regions. The regions close to the precursor inlet are still uniformly covered, whereas the opposite part of the wafer has much thinner film. The thickness difference between maximum and minimum is up to 30nm. These indicate that the underdose occurs and the thickness variation is 60%.

9 Conclusions

In this work, the relationship among precursor pulse length, pulse mode, film growth rate, uniformity, and thickness profile has been studied. The investigation is important for a basic understanding of precursor pulsing effect on ALD film growth and properties, and also for future applications on non-flat substrates, such as porous materials and large surface.

The results form modeling and simulation of TMA pulse show that the pressure in the tube decreases to a steady state when pulse valve is open. When the valve is close, this pressure increases to the original level with nearly the same time as the pressure decreasing. However, the pressure in the precursor cylinder does not change very much due to the high vapor pressure of TMA. The pressure in precursor cylinder is much higher than that in reaction chamber so that TMA can be pulsed efficiently. Consequently, hundred seconds pulse for porous materials can be progressed.

The result from the growth of Al_2O_3 and Ta_2O_5 films indicates that the precursor pulse length is a very important parameter to optimize precursor dose, which finally affects the film growth rate, mean thickness and thickness variations. Non-uniformity thickness profiles could be results of precursor underdose or overdose. If the precursor pulse time

is too long and purge time is too short, the non-uniformity is contributed by the remarkable CVD reaction for Al_2O_3 and etching reaction for Ta_2O_5.

The result from optimization of pulse mode showed that, for low vapor pressure solid precursor, standard pulse mode and assistant flow pulse mode do not work. In overflow pulse mode, although film can be attained but at low growth rate, small mean thickness and poor uniformity indicate that precursor is not pulsed effectively. The result from booster pulse with standard pulse mode is similar to that from combination pulse mode.

In the future, the work will concentrate on non-flat substrate with the advantage of conformal ALD, such as round surface of optical fiber, porous materials and large three dimension surface. The work should also involve the modeling and simulation for low vapor pressure precursor, such as solid $TaCl_5$，$Er(thd)_3$, $HfCl_4$ and $Yb(thd)_3$. Long pulse length at hundred-second level will be carried out in experiments to increase the precursor penetration into porous materials.

References

[1] R. L. Puurunen, J. App. Phys. **97**, (2005) 121301.

[2] M. Knez, K. Nielsch, L. Niinistö, Adv. Mater. 2007, **19**, 3425-3438.

[3] T. Suntola and J. Antson, US Pantent 4058430 (1977).

[4] L. Niinistö, J. Päiväsaari, J.Niinistö, M. Putkonen, M. Nieminen, Phys. Stat. Sol. **201**, No. 7, (2004) 1443-1452.

[5] M. Leskelä, M. Ritala, Thin Solid Films **409** (2002) 138-146.

[6] C. Chaneliere, J.L. Autran, R.A.B. Devine, B. Balland, Mater. Sci. Eng., R.22, (1998) 269.

[7] D. Riihelä, M. Ritala, R. Matero, M. Leskelä, Thin Solid Films **289,** (1996) 250-255.

[8] M. Ritala, Markku Leskelä, Handbook of Thin Film Materials, edited by H. S. Nalwa (Academic, San Diego, 2002) Vol. 1, pp. 103-159.

[9] A. Martin Hoyas, J. Schuhmacher, D. Shamiryan, J. Waeterloos, W. Besling, J. P. Celis, K. Maex, J. Appl. Phy. **95**, (2004) 381.

[10] S. Haukka, E. L. Lakomaa, T. Suntola, Stud. Surf. Sci. Catal. **120**, (1998) 715.

[11] S. M. George, A. W. Ott, J. W. Klaus, J. Phy. Chem. **100**, (1996) 13121.

[12] M. Ylilammi, Thin Solid Films **279**, (1996) 124.

[13] R. L. Puurunen, Chem. Vap. Deposition **9**, (2003) 249.

[14] D. H. Everett, Pur. Appl. Chem. **31**, (1972) 579.

[15] T. Suntola, Mater. Sci. Rep. **4**, (1989) 261.

[16] L. Niinistö, M. Leskelä, Thin Solid Films **225**, (1993) 130.

[17] R. L. Puurunen, Chem. Vap. Deposition **9**, (2003) 327.

[18] M. Putkonen, T. Sajavaara, L. S. Johansson, L. Niinistö, Chem. Vap. Deposition **7**, (2001) 44.

[19] T. Pilvi, Academic dissertation, ISBN 978-952-92-4814-8, Yliopistopaino, Helsinki 2008.

[20] J. Aarik, K Kukli, A Aidla, L. Pung, Applied Surface Science **103** (1996) 331-341.

[21] Anthony C. Jones, Michael J. Hitchman,Chemical Vapour Deposition, Royal Society of Chemistry, 2008.

[22] P. Atkins, Physical Chemistry, Oxford University Press, 1982.

[23] A. Roth, Vacuum Technology, North Holland, 1986.

[24] R. Glang, Handbook of Thin Film Technology, Mc Graw Hill, 1970.

[25] H. Fujiwara, Spectroscopic Ellipsometry: Principle and Application, 2007 John Wiley & Sons, Ltd.

[26] R. M. A Azzam, Optics Letters, Vol.32, No.3(2009).

[27] Micronova website, http://micronova.tkk.fi/equipment/ellipsometer.html

[28] AIR LIQUIDE website, © Copyright AIR LIQUIDE 2007, http://encyclopedia.airliquide.com/Encyclopedia.asp?GasID=69.

[29] I. Eames, N. Marr, H. Sabir, International J. of Heat and Mass transfer, Vol. 40, (1997)12

[30] R. Matero, A. Rahtu, M. Ritala, M. Leskelä, T. Sajavaara, Thin Solid Films **368** (2000) 1-7.

[31] K. An, W. Cho, K. Sung, S. S. Lee, Y. Kim, Bull. Korean Chem. Soc. 2003, vol. **24**, No. 11.

[32] K. Kukli, M. Ritala, R. Matero, M. Leskelä, J. Crys. Grow. **212** (2000) 459-468.

[33] H. Simon, J. Aarik, J. Phys. D: Appl. Phys. **30** (1997) 1725-1728.

[34] M. Ritala, M. Leskelä, E. Nykänen, P. Soininen, L. Niinistö, Thin Solid Films **225**, (1993) 288.